OFFPRINT

Height fluctuations of a contact line: A direct measurement of the renormalized disorder correlator

P. LE DOUSSAL, K. J. WIESE, S. MOULINET and E. ROLLEY

Please visit the new website
www.epljournal.org

Height fluctuations of a contact line: A direct measurement of the renormalized disorder correlator

P. Le Doussal[1(a)], K. J. Wiese[1(b)], S. Moulinet[2,3(c)] and E. Rolley[2(d)]

[1] *CNRS-Laboratoire de Physique Théorique de l'Ecole Normale Supérieure - 24 rue Lhomond, 75005 Paris, France, EU*
[2] *Laboratoire de Physique Statistique, (ENS, CNRS, Universités Paris 6 et Paris 7) - 24 rue Lhomond, 75005 Paris, France, EU*
[3] *Laboratoire Jean Perrin (CNRS, Université Paris 6) - 24 rue Lhomond, 75005 Paris, France, EU*

Abstract – We measure the center-of-mass fluctuations of the height of a contact line at depinning for two different systems: liquid hydrogen on a rough cesium substrate and isopropanol on a silicon wafer grafted with silanized patches. The contact line is subject to a confining quadratic well, provided by gravity. From the second cumulant of the height fluctuations, we measure the renormalized disorder correlator $\Delta(u)$, predicted by Functional RG to attain a fixed point, as soon as the capillary length is large compared to the Larkin length set by the microscopic disorder. The experiments are consistent with the asymptotic form for $\Delta(u)$ predicted by Functional RG, including a linear cusp at $u = 0$. The observed small deviations could be used as a probe of the underlying physical processes. The third moment, as well as avalanche-size distributions are measured and compared to predictions from Functional RG.

A direct measurement of the fixed-point function $\Delta(u)$, the so-called renormalized disorder correlator, which plays a central role in the Functional RG (FRG) of pinned elastic systems, was recently proposed [1] and verified in an exact numerical determination of ground states for interfaces in various types of disorders [2]. The main idea is to put the elastic system in a quadratic potential well, which acts as a large-scale cutoff and makes the problem well defined. The shift between the center of mass and the center of the well is proportional to the renormalized force and its fluctuations are the quantity computed in the FRG [1]. The results of [2] show a remarkable agreement in the statics between the measured $\Delta(u)$ and the 1- and 2-loop predictions from the Functional RG [3–5]. These ideas and numerical tests have been extended to the depinning transition [6,7] in the case of local elasticity, and to reaction diffusion models [8]. Finally, a first-principle calculation of the distribution of avalanches from the FRG was performed and verified by numerics [9–11]. An outstanding challenge is to test these predictions in experiments.

The depinning of the contact line of a fluid on a disordered substrate has been studied experimentally [12–15] and its critical scaling established. Since gravity creates a quadratic well, this raises the interesting possibility of measuring a FRG fixed-point function for depinning or, conversely, to learn more about the physical system using these (universal) fluctuations as a probe. To do so, the capillary length, which provides the well, does not need to be larger than the measurement scale. In fact, the finite capillary length is used as an advantage.

Consider a fluid in a large reservoir and its contact line (CL) on a plate, parameterized by $(x, u(x))$ within the plate (fig. 1). Its energy can be modeled as

$$\mathcal{H}[u] = \int_0^L \mathrm{d}x \, \frac{m^2}{2} \left[u(x) - w \right]^2 + V(x, u(x)) + \mathcal{E}[u], \quad (1)$$

where $\mathcal{E}[u]$ is a non-local elastic energy invariant under $u(x) \to u(x) + \text{const}$. The pinning force $-\partial_u V(x, u)$ is a local quenched random function. L is the total length of the contact line. Additional boundary terms, not written here, affect the line near $x = 0$ and $x = L$. The position w of the center of the well with respect to the plate, which is also the equilibrium position of the CL without disorder, is fixed by the height w_∞ in the reservoir far away

(a)E-mail: ledou@lpt.ens.fr
(b)E-mail: wiese@lpt.ens.fr
(c)E-mail: moulinet@lps.ens.fr
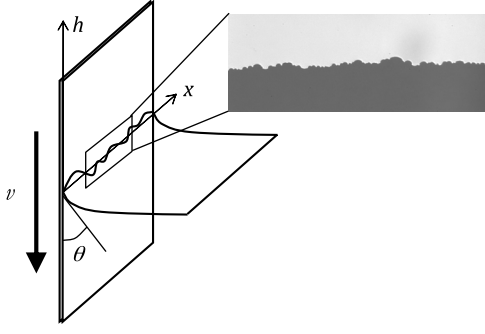(d)E-mail: etienne.rolley@lps.ens.fr

Fig. 1: Sketch of the experimental setup. The size of the image in the inset is 1.5 mm.

from the contact line, up to a constant shift $w = w_\infty + \sqrt{2}L_c\sqrt{1 - \sin\theta}$, where $L_c = \sqrt{\gamma/\rho g}$ is the capillary length and θ the contact angle. In the simplest model of the fluid surface the elastic energy $\mathcal{E}[u]$ in Fourier space is $\mathcal{E}[u] = \frac{1}{2}\int\frac{\mathrm{d}k}{2\pi}\epsilon_k u_{-k}u_k$, with an elastic kernel $\epsilon_k = m^2\tilde{\epsilon}_\theta(k/k_\theta)$. The curvature of the quadratic well is $m^2 = \gamma k_\theta$ with $k_\theta = \sqrt{2}\sin(\theta)/(L_c\sqrt{1+\sin\theta})$. The scaling function $\epsilon_\theta(x)$ is often approximated by $\tilde{\epsilon}_{\pi/2}(x) = \sqrt{x^2+1} - 1$, but can be computed for any θ [16].

One drives the system by slowly immersing the plate at a constant velocity v, hence $w = vt$. The center of mass $\bar{u}(t) := \frac{1}{L}\int_0^L \mathrm{d}x\, u(x,t)$ is fluctuating as a function of w, and contains valuable information about the system. In particular, the second cumulant $\Delta(w)$, defined as

$$\Delta(vt) := Lm^4\langle[\bar{u}(t+\tau) - v(t+\tau)][\bar{u}(\tau) - v\tau]\rangle^c \qquad (2)$$

with $w = vt$ is exactly the renormalized disorder correlator computed by the FRG theory. Here and below $\langle\ldots\rangle$ denotes translational averages in the direction of the motion of the CL. Thus a direct measurement of $\Delta(w)$ is possible for the CL moving on a disordered substrate.

Two different systems have been used. The first one is liquid hydrogen on a cesium substrate, denoted H$_2$/Cs. As in most previous experiments using H$_2$/Cs, the Cs substrate is prepared at low temperature, yielding a rough surface with dense defects whose size is of the order of $10\,\mathrm{nm}$ [12,13]. Such a small value leads to very small distortions of the CL and precludes any optical observation. We have thus annealed the Cs layer up to $250\,\mathrm{K}$. This creates a large-scale structure (possibly corrugation) which is visible but cannot be characterized since its typical length scale is in the micrometer range, below optical resolution.

The second system is isobutanol on a silicon wafer, denoted iso/Si. We create a well-controlled disorder by photolithographic techniques: the Si wafer is decorated by random silanized square patches $(10 \times 10\,\mu\mathrm{m}^2)$ (see footnote [1]) which cover about 22% of the total area. As the silanized patches are less wettable than Si, each patch can pin the CL.

---

[1]Silanization is done in the vapor phase, using 1H,1H,2H,2H-Perfluorodecyltrichlorosilane from Alfa Aesar GmbH&Co KG.

Table 1: Wetting properties.

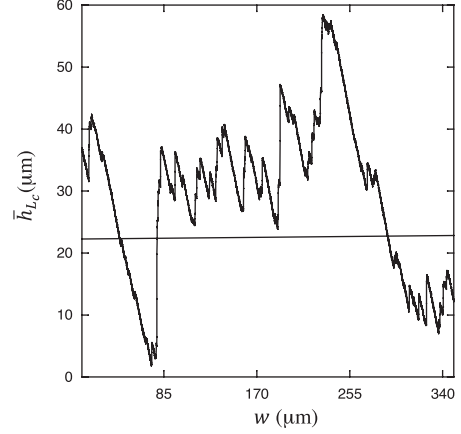|	θ (degrees)	γ (mN/m)	L_c (mm)	η (mPa$\cdot$s)
H$_2$ at 15 K	~ 40	2.79	1.94	0.021
Isobutanol	~ 40	20.9	1.64	4.0

Fig. 2: Height of the contact line $\bar{h}_{2L_c}(w)$ averaged over $2L_c$, as a function of the position w of the plate (system: iso/Si). The fast depinning events (upwards) are clearly visible. Between them, the CL is advected downwards at the plate velocity v (here $1\,\mu\mathrm{m/s}$). The straight line is the reference level h_0.

The relevant parameters (advancing contact angle θ, liquid-vapor surface tension γ, capillary length L_c and dynamic viscosity η) are listed in table 1 for both systems. Note that contact angle and capillary length are similar. In both systems defects are strong so that the Larkin length is set by the size ξ of the defects; ξ is macroscopic so that thermal activation is irrelevant [12].

A sketch of the experimental setup is shown in fig. 1. The substrate is dipped into the liquid at constant velocity v. The CL is imaged with a standard progressive-scan CCD camera for velocities up to $10\,\mu\mathrm{m/s}$. At room temperature we have also used a high-speed camera in order to analyse the CL dynamics up to $v = 1200\,\mu\mathrm{m/s}$. For each time t, the CL profile is digitized to obtain the CL height $h(x,t)$. The correspondence with the above notations is

$$h(x,t) - h_0 = u(x,t) - vt\ - \langle u(x,t) - vt\rangle. \qquad (3)$$

To define the reference level h_0 we first calculate the average height $\bar{h}_l(t)$ over a CL length l: $\bar{h}_l(t) := \frac{1}{l}\int_0^l h(x,t)\,\mathrm{d}x$. An example is shown in fig. 2. Then h_0 is obtained as the time-averaged value of $\bar{h}_l(t)$. As the camera is fixed with respect to the liquid container, one expects h_0 to be constant. However, we allow for a slow drift of h_0 for two reasons: first, as the volume of the container is finite, dipping the plate causes a slight increase of the asymptotic level which results in a linear increase of the reference level h_0. Secondly, the slow variations of $\bar{h}_l(t)$ are not linear, due to large-scale variations
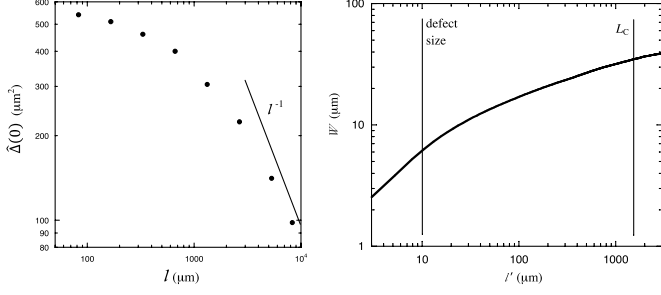
Fig. 3: Left: scaling of the correlator $\hat{\Delta}(0) := \langle \bar{h}_l(w)\bar{h}_l(w)\rangle$ as a function of the averaging length l along the CL (here iso/Si). The asymptotic scaling l^{-1} is marginally reached for $l = L_c$. Right: roughness $W(l')$ of the contact line for iso/Si. Due to the limited range between the defect size and the capillary length, no scaling is achieved.

of the plate properties (defect size, mean contact angle, etc.). Hence, $h_0(t)$ is determined experimentally by fitting the data set $\bar{h}_l(t)$ by a polynomial. As we are interested in correlations over distances two orders of magnitude smaller than the total swept distance, this only shifts the correlator Δ by a constant.

In the following, instead of $h(x,t)$, we use $\mathsf{h}(x,w) := h(x,w/v) - h_0$, where $w = vt$, making it easier to compare runs at different velocities v. We define the experimentally measured correlator $\hat{\Delta}$ as

$$\hat{\Delta}(w - w') := \langle \bar{\mathsf{h}}_l(w)\bar{\mathsf{h}}_l(w')\rangle. \tag{4}$$

We need to choose the CL length l over which h is averaged. It must be larger than the capillary length L_c, and as large as possible, while remaining notably smaller than the plate size $L \approx 20\,\mathrm{mm}$, since strong distortions occur at the edge of the plate. Moreover, slow changes of the plate properties cause slow variations of the capillary rise on the plate. These are small compared to the fluctuations of the *local* CL height, but one expects that $\hat{\Delta}$ varies like l^{-1} (for $l \gg L_c$). So, the larger l, the stronger the effect of the large-scale heterogeneities. As a compromise, we have chosen $l = 2L_c$. As shown in fig. 3, $\hat{\Delta}(0)$ has almost reached the asymptotic behavior for $l = 2L_c$. Once l is chosen, an accurate determination of $\hat{\Delta}(w' - w)$ requires that the CL explore a large number of pinned configurations, *i.e.* the CL has to sweep a range of w much larger than the width of the line. Following [14,15], we define the CL width W at scale l' as $W^2(l') = \langle((h(x,t) - h(x + l',t))^2\rangle$, where the average is taken over x and over all successive configurations. For iso/Si, we find a width $W \simeq 40\,\mu\mathrm{m}$ for $l' \gtrsim 2L_c$; for H_2/Cs, the width is much smaller and difficult to measure, but we estimate that $W \approx 5\,\mu\mathrm{m}$ at large scale. The CL sweeps about $80\,\mathrm{mm}$ for iso/Si and about $5\,\mathrm{mm}$ for H_2/Cs. The plate displacement is thus much larger than W. This is necessary in order to get a reproducible shape for Δ. As a consequence, the disorder and the substrate properties have to be fairly homogeneous over an area of at least $1\,\mathrm{cm}^2$, which is quite difficult to achieve. In particular,
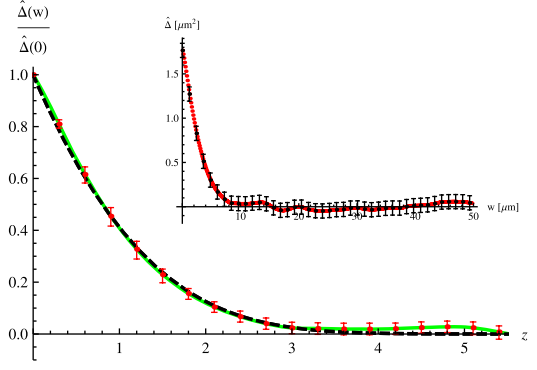

Fig. 4: (Colour on-line) Inset: the disorder correlator $\hat{\Delta}(w)$ for H_2/Cs, with error bars estimated from the experiment. Main plot: the rescaled disorder correlator $\hat{\Delta}(w)/\hat{\Delta}(0)$ (green solid line) with error bars (red). The dashed line is the 1-loop result from eq. (5).

Fig. 5: (Colour on-line) Inset: the disorder correlator $\hat{\Delta}(w)$ for iso/Si at $v = 1\,\mu\mathrm{m/s}$ up to $w = 35\,\mu\mathrm{m}$, and then at $v = 10\,\mu\mathrm{m/s}$ for $w > 35\,\mu\mathrm{m}$, with error bars as estimated from the experiment. Main plot: the rescaled disorder correlator $\hat{\Delta}(w)/\hat{\Delta}(0)$ (green solid line) with error bars (red). The dashed line is the 1-loop result (5).

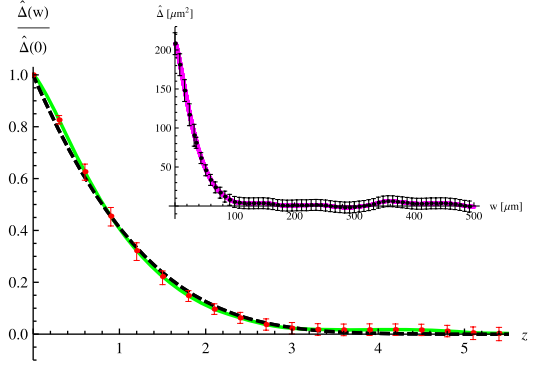we have first tried to use water on glass decorated with Cr defects as in [14], but we could not get rid of strong variations of the capillary rise.

When comparing the two systems used in this work, the main difference lies in the defect size ξ, which is roughly one order of magnitude smaller for H_2/Cs compared to iso/Si. The drawback of the low-temperature system is the poor characterization of the disorder which cannot be resolved optically. But the small value of ξ is rather an advantage as the separation between the small-scale cut-off ξ (defect size) and the large-scale cut-off L_c (capillary length) is about 3 orders of magnitude for H_2/Cs, while only about 2 for iso/Si. As a consequence, it is difficult to observe the scaling regime for iso/Si. For instance, $W(l')$ does not exhibit scaling in fig. 3. The case of H_2/Cs is closer to previous experiments of the same type which did exhibit scaling.

We now discuss our experimental results and their comparison to theory. The raw data for the correlator $\hat{\Delta}(w)$ defined in (4) are shown in the insets of figs. 4 and 5. To compare with theory it is useful to define
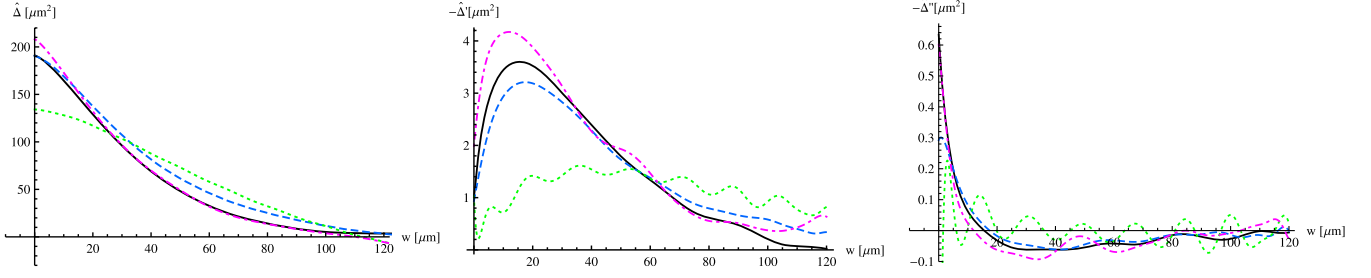
Fig. 6: (Colour on-line) The disorder correlator $\hat{\Delta}(u)$ (left), and (minus) its first (middle) and second (right) derivatives. The velocities are $v = 1\,\mu\mathrm{m/s}$ (dash-dotted pink line), $v = 10\,\mu\mathrm{m/s}$ (solid black line), $v = 100\,\mu\mathrm{m/s}$ (blue dashed line) and $v = 1200\,\mu\mathrm{m/s}$ (green dotted line). Statistical errors for $\Delta'(w)$ are $\approx 5\%$. (The derivatives are obtained by fitting with a polynomial of degree 50 to 100 for $0 \leqslant w \leqslant 120$.) The non-zero value of $\hat{\Delta}'(0^+)$ is the signature of the predicted linear cusp.

a dimensionless disorder correlator as in [2] and plot the ratio $Y := \hat{\Delta}(w)/\hat{\Delta}(0)$ as a function of the variable z with $w = z \int_0^\infty \mathrm{d}w'\, \hat{\Delta}(w')/\hat{\Delta}(0)$ so that the area under the curve is unity. The resulting function has no free parameter and the functional RG theory of pinned systems predicts that in the limit of small m: i) it should be the same function for all systems in a given universality class (UC); ii) this function should exhibit a linear cusp near $w = 0^+$. In figs. 4 and 5 we have plotted these dimensionless correlators (solid lines).

Also shown in figs. 4 and 5 is the 1-loop prediction

$$z = \sqrt{Y_{1\text{-loop}} - 1 - \ln Y_{1\text{-loop}}} \Big/ \int_0^1 \mathrm{d}y\, \sqrt{y - 1 - \ln y} \quad (5)$$

for the universality class described by eq. (1), *i.e.* quasi-static depinning with irrelevant non-linear terms, the only class for which this function has been computed analytically yet. One sees a very good agreement between data and 1-loop FRG prediction. A similar agreement was observed numerically both in the statics and the dynamics of pinned systems with *local* elasticity [2,7]. At this stage we take this as a clear signature for a pinned system, and that a description using eq. (1) is possible. A significantly higher precision and statistics (of a factor ≈ 10–20) would be required to reach the one achieved in numerics [2,7]. That would provide a decisive test on the universality class, and shed light on the debate about the large observed value for $\zeta \approx 0.5$ [15], while analytical predictions based on model (1) lie around $\zeta = 0.4$ [4,17]. Closer examination of the data in fig. 5 shows that deviations from $Y_{1\text{-loop}}(z)$ can be mainly accounted for by rounding, which thus must be better controlled and quantified.

For iso/Si, we have performed the experiment at different velocities, in order to see the approach to the fixed point, and check for experimental artifacts. This is shown in fig. 6. We first comment on the shape of the correlator at the highest velocity ($v = 1200\,\mu\mathrm{m/s}$). The flattening at the origin is expected as the system is driven away from the depinning threshold (*i.e.* away from the fixed point). However the large oscillations in $\hat{\Delta}(w)$ (better visible in its derivative) are surprising. We believe

them to be due to surface waves of the liquid, possibly excited by the motor moving the plate. Decreasing the velocity, the cusp at the origin becomes more and more pronounced, though even at the lowest velocity $v = 1\,\mu\mathrm{m}$ the first derivative $\hat{\Delta}'(w)$ is not yet monotonically decreasing, as predicted by theory for $v = 0^+$.

One possible origin of the observed rounding may be that the dissipation is not simply due to viscous shear in the meniscus but involves complex microscopic processes at the solid surface. This is suggested by the fact that the behavior of the correlator for vanishing z is sensitive to the cleaning procedure of the plate, and by the fact that the homogeneous bare silicon surface displays an *intrinsic* hysteresis (for a discussion, see [18]). At this stage, we have little idea how the underlying microscopic disorder could change the behavior of the CL at the scale of the macroscopically patterned defects, and how to predict the possible resulting rounding effect.

On the other hand, there are also two fundamental reasons why the system could be slightly off the fixed point: i) rounding by the velocity, as observed above and expected from the theory (although most models predict that $\Delta'(0^+) = 0$ at $v > 0$; this point is still debated [19]) ii) as suggested by the width data in fig. 3, the ratio ξ/L_c (or equivalently m) is yet too large to have reached the fixed point. The shape of $\hat{\Delta}'(w)$ is qualitatively what is expected: $\hat{\Delta}'(0^+)$ is strictly positive, hence the system is above the Larkin scale, but it is significantly smaller than its putative fixed-point value, since $\hat{\Delta}'(w)$ should be monotonically decaying there. Similarly $\hat{\Delta}''(w) < 0$ near $w = 0$ while the fixed-point value is expected to be positive. This interpretation, if confirmed, is interesting, as it implies that $\hat{\Delta}(w)$ is a sensitive new probe, which can be made quantitative, to test how far the system is from criticality.

More information can be obtained from the experimental data by computing the third cumulant

$$\hat{S}_3(w - w') := \langle [\mathsf{h}_l(w) - \mathsf{h}_l(w')]^3 \rangle. \quad (6)$$

It is convenient to plot the function

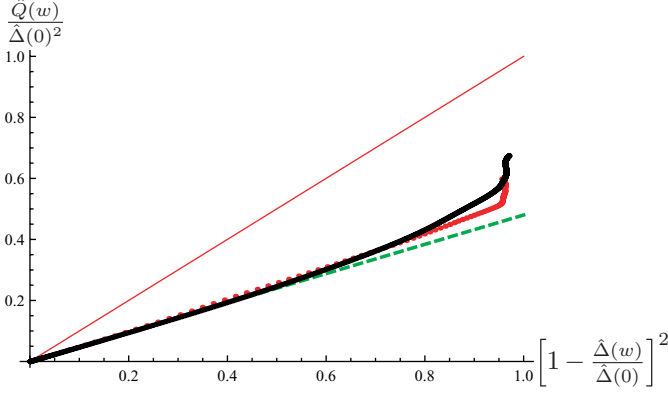$$\hat{Q}(w) := \frac{1}{6} \int_0^w \mathrm{d}w'\, \hat{S}_3(w'). \quad (7)$$

Fig. 7: (Colour on-line) Dimensionless parametric plot of $\hat{Q}(w)/\hat{\Delta}(0)^2$ *vs.* $[1 - \frac{\hat{\Delta}(w)}{\hat{\Delta}(0)}]^2$ for both experiments H_2/Cs (thick red line) and iso/Si at $v = 10\,\mu m/s$ (thick black line). The thin red line is the mean-field prediction. The thick dashed green line is an extrapolation based on a loop expansion, as discussed in the text.

Indeed, the FRG predicts that

$$\frac{\hat{Q}(w)}{\hat{\Delta}(0)^2} \approx A \left[1 - \frac{\hat{\Delta}(w)}{\hat{\Delta}(0)} \right]^2, \qquad (8)$$

with an exact equality and the universal amplitude $A = 1$ at the mean-field level (*i.e.* resummation of tree diagrams, $d \geqslant d_{uc} = 2$). The proportionality (with no attempt to measure A) was checked numerically [7] for depinning with *local* elasticity. In fig. 7 we plot both sides of eq. (8): we see that the proportionality holds very nicely and that the two experiments fall on top of each other, confirming the universality of the slope A, which is measured to be $A \approx 0.53$. The FRG calculation, using the scaled elastic kernel $\tilde{\epsilon}_{\pi/2}(x)$ yields $A = 1/(1 + \frac{8}{9}\epsilon) + O(\epsilon^2)$ with $\epsilon = 2 - d$ (see (E12) of [10]) which yields $9/17 = 0.53$ and 0.11 for the two Padé approximants at $\epsilon = 1$, while the kernel $\tilde{\epsilon}_\theta(x)$ with $\theta = 40°$ gives [16] $A = 0.48 \pm 0.13$ (shown in fig. 7). These values are reasonable, given that the correction to mean field is large and one cannot hope for high precision. Also note that deviations from the functional form in eq. (8) are expected at 1-loop order, but they should be small as found numerically in [7]. We conclude that the agreement between experiment and theory is satisfactory for the third cumulant.

The properties of the CL can also be characterized by the distribution of the sizes S of avalanches, or forward jumps (see fig. 2), where by definition S is the area swept during the avalanche. At the critical point, $m = 0$, the distribution is expected to be a power law characterized by an exponent τ. At small $m > 0$, the correlation length is finite and the avalanche-size distribution $P(S)$ for $S \gg S_{min}$ is cut off at scale

$$S_m := \frac{\langle S^2 \rangle}{2\langle S \rangle}, \qquad (9)$$

where here and below $\langle \ldots \rangle$ denotes an average over $P(S)$. One expects that in the variable $s := S/S_m$ the avalanche-size distribution exhibits universality, *i.e.* independence from short scales, and that, for $1 < \tau < 2$, it takes the form

$$P(S)\mathrm{d}S := \frac{\langle S \rangle}{S_m} p\left(\frac{S}{S_m} \right) \frac{\mathrm{d}S}{S_m}. \qquad (10)$$

The function $p(s)$ is universal, and by construction from (9) and (10) normalized such that $\int_0^\infty \mathrm{d}s\, s p(s) = 1$ and $\int_0^\infty \mathrm{d}s\, s^2 p(s) = 2$ (see footnote [2]). The analytical prediction [10] for $p(s)$ reads, based on the model (1) and with the scaled elastic kernel $\tilde{\epsilon}_{\pi/2}(x)$,

$$p(s) = A' s^{-\tau} \exp\left(-\frac{B'}{4} s^{\delta'} + C'\sqrt{s} - D' s^{\frac{3}{2}} \right) \qquad (11)$$

with $B' = 1 + \frac{1}{3}(\gamma - 2)\epsilon$, $C' = \frac{\sqrt{\pi}\epsilon}{3}$, $D' = \frac{\sqrt{\pi}\epsilon}{36}$, A' given by the normalization and the exponent $\delta' = 1 + \frac{\epsilon}{3}$. This prediction is exact to first order in $\epsilon = 2 - d$, and to produce our analytical estimate we set $\epsilon = 1$ and rescale both axes to ensure the two normalization conditions. For the τ-exponent, we have used the conjectured relation $\tau(\zeta) = 2 - 1/(d + \zeta)$ since we proved [10] that the latter is exact at least to one loop. Inserting the measured $\zeta \approx 0.5$ yields the prediction $\tau \approx 4/3$.

The size distribution is measured only for iso/Si with a standard camera (acquisition rate: 15 Hz), at a velocity $v = 1\,\mu m/s$. We consider that an event occurs if the local displacement between two successive images is larger than a threshold $\delta h \simeq 8\,\mu m$. This threshold is about the defect size, which is the smallest displacement occurring in an avalanche, and is about 10 times larger than the resolution on the CL position. The area S swept in a single avalanche is then computed as the sum of the displacements occurring before the CL is pinned again. We detected 16×10^3 avalanches for a swept area of $3.5 \times 20\,mm^2$. We have checked that the resulting distribution is not sensitive to the value of the threshold and that the acquisition rate is fast enough to avoid lumping together uncorrelated avalanches.

Experimental data and predictions are shown in fig. 8. We see that the parameter-free scaling collapse is quite good down to $s = 10^{-2}$. This value of s corresponds to $S = 100\,\mu m^2$, which is the cutoff expected from the size of the defects whose area is $100\,\mu m^2$. However, our accuracy is limited by the available sizes, and *e.g.* not sufficient to discriminate between $\tau(\zeta = 0.5) = 4/3$, and $\tau(\zeta = 0.4) = 1.29$. While $p(s)$ has strong statistical fluctuations, the characteristic function

$$\tilde{Z}(\lambda) := \int_0^\infty \mathrm{d}s\, p(s) \left(e^{\lambda s} - 1 \right) \qquad (12)$$

can be measured quite accurately as shown in fig. 9. The 1-loop extrapolation ($\epsilon = 1$) is closer to the data than mean

---

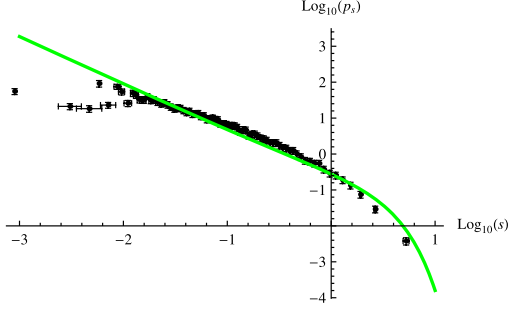[2] $p(s)$ is itself *not* a probability distribution, since $\int \mathrm{d}s\, p(s) \neq 1$.

Fig. 8: (Colour on-line) The measured dimensionless avalanche-size distribution function $p(s)$, as defined in the text, for iso/Si. For comparison an analytical estimate, defined in eq. (11), based on a one-loop calculation with the scaled elastic kernel $\tilde{\epsilon}_{\pi/2}(x)$. The small-size cutoff is $\log_{10}(s) = -2$, *i.e.* the size of a defect.
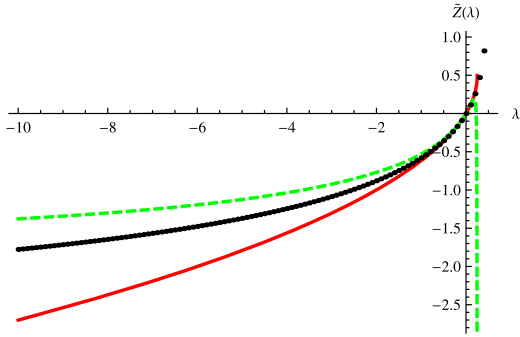

Fig. 9: (Colour on-line) $\tilde{Z}(\lambda)$ defined in (12), from bottom to top: the mean-field prediction (red solid line), the experimental data (black dots), and the extrapolation based on the one-loop calculation for a scaled elastic kernel $\tilde{\epsilon}_{\theta}(x)$ with $\theta = 40°$ (green dashed line).

field and using the elasticity $\tilde{\epsilon}_{\theta=40°}(x)$ (shown in fig. 9) is closer than with $\tilde{\epsilon}_{\theta=\pi/2}(x)$ (not shown). Hence comparison to field-theory [10,16] is satisfactory.

We now come to a final test of the avalanche picture underlying the FRG calculations. According to [9,10], the slope $\hat{\Delta}'(0^+)$ of the linear cusp is proportional to the scale S_m of the avalanche-size distribution,

$$L \left| \hat{\Delta}'(0^+) \right| = S_m \equiv \frac{\langle S^2 \rangle}{2 \langle S \rangle}. \tag{13}$$

We find $S_m \simeq 9000 \, \mu\text{m}^2$. At the lowest velocity, $|\hat{\Delta}'(0^+)| = 1.75 \, \mu\text{m}^2$, $L = 3500 \, \mu\text{m}$, thus $L|\hat{\Delta}'(0^+)| \simeq 6100 \, \mu\text{m}^2$. However, estimating $\hat{\Delta}'(0^+)$ is difficult because we do not understand the origin for the rounding of $\hat{\Delta}(w)$ when $w \to 0$. An upper bound for $|\hat{\Delta}'(0^+)|$ is the slope of $\hat{\Delta}'$ at the inflection point, which yields $L|\hat{\Delta}'(0^+)| < 14000 \, \mu\text{m}^2$. The third moment of S can similarly be related to the third cumulant of the center-of-mass fluctuations: $\langle S^3 \rangle \langle S \rangle / (3 \langle S^2 \rangle^2) = A$, with A defined in eq. (8). From $p(s)$ we find $A = 0.77$, while the relation between $\hat{Q}(w)$ and $\hat{\Delta}(w)$ yields $A = 0.53$. The agreement in both cases is only fair and more experiments are needed. In particular, a smaller ratio ξ/L_c would be helpful.

To conclude: by examining the fluctuations of the mean height of the contact-line at depinning, we have measured the renormalized disorder-correlator $\Delta(w)$. The latter is the central object of the functional RG field theory, and its predicted cusp, which is the sign of metastability, shocks and avalanches, was under intense debate from the field theory side. Here we have made the first comparison between experiment and theory. It shows qualitatively and quantitatively that the ideas in the latter are correct, and opens new ways of quantifying the former, calling for new experiments.

$* * *$

REFERENCES

[1] LE DOUSSAL P., *Europhys. Lett.*, **76** (2006) 457, cond-mat/0605490; arXiv:0809.1192.
[2] MIDDLETON A. A., LE DOUSSAL P. and WIESE K. J., *Phys. Rev. Lett.*, **98** (2007) 155701.
[3] FISHER D. S., *Phys. Rev. Lett.*, **56** (1986) 1964.
[4] CHAUVE P., LE DOUSSAL P. and WIESE K. J., *Phys. Rev. Lett.*, **86** (2001) 1785; LE DOUSSAL P., WIESE K. J. and CHAUVE P., *Phys. Rev. B*, **66** (2002) 174201.
[5] NATTERMANN T. *et al.*, *J. Phys. II*, **2** (1992) 1483; NARAYAN O. and FISHER D. S., *Phys. Rev. B*, **48** (1993) 7030.
[6] LE DOUSSAL P. and WIESE K. J., *EPL*, **77** (2007) 66001.
[7] ROSSO A., LE DOUSSAL P. and WIESE K. J., *Phys. Rev. B*, **75** (2007) 220201.
[8] BONACHELA J. A., ALAVA M. and MUNOZ M. A., *Phys. Rev. E*, **79** (2009) 050106(R).
[9] LE DOUSSAL P., MIDDLETON A. A and WIESE K. J., *Phys. Rev. E*, **79** (2009) 050101(R).
[10] LE DOUSSAL P. and WIESE K. J., *Phys. Rev. E*, **79** (2009) 051106.
[11] ROSSO A., LE DOUSSAL P. and WIESE K. J., arXiv:0904.1123.
[12] ROLLEY E. and GUTHMANN C., *Phys. Rev. Lett.*, **98** (2007) 166105.
[13] ZECH M., FUBEL A., LEIDERER P. and KLIER J., *J. Low Temp. Phys.*, **137** (2004) 179.
[14] MOULINET S., GUTHMANN C. and ROLLEY E., *Eur. Phys. J. E*, **8** (2002) 437.
[15] MOULINET S., ROSSO A., KRAUTH W. and ROLLEY E., *Phys. Rev. E*, **69** (2004) 035103.
[16] LE DOUSSAL P. and WIESE K. J., arXiv:0908.4001.
[17] ROSSO A., HARTMANN A. K. and KRAUTH W., *Phys. Rev. E*, **67** (2003) 021602, cond-mat/0207288.
[18] MOULINET S., GUTHMANN C. and ROLLEY E., *Eur. Phys. J. B*, **37** (2004) 127.
[19] CHAUVE P., GIAMARCHI T. and LE DOUSSAL P., *Phys. Rev. B*, **62** (2000) 6241.